Incorporating microbial dormancy dynamics into soil decomposition models to improve quantification of soil carbon dynamics of northern temperate forests

Yujie He[1], Jinyan Yang[2,3], Qianlai Zhuang[1,4], Jennifer W. Harden[5], Anthony D. McGuire[6], Yaling Liu[1], Gangsheng Wang[7], Lianhong Gu[7]

(1) Department of Earth, Atmospheric, and Planetary Sciences, Purdue University, West Lafayette, Indiana, USA

(2) Warnell School of Forestry and Natural Resources, University of Georgia, Athens, GA 30605, USA

(3) Center for Ecological Research, Northeast Forestry University, Harbin 150040, China

(4) Department of Agronomy, Purdue University, West Lafayette, Indiana, USA

(5) U.S. Geological Survey, 345 Middlefield Rd, Menlo Park, MS 962, CA 94025, USA

(6) U.S. Geological Survey, Alaska Cooperative Fish and Wildlife Research Unit, University of Alaska Fairbanks, Fairbanks, Alaska, USA

(7) Climate Change Science Institute and Environmental Sciences Division, Oak Ridge National Laboratory, Oak Ridge, Tennessee, USA

Corresponding author: Qianlai Zhuang. Address: 550 Stadium Mall Drive, West Lafayette, IN, 47907-2051, United States. Tel.: + 1 765 494 9610. E-mail: qzhuang@purdue.edu

Running Title: modeling microbial dormancy in global temperate forest ecosystem

Abstract

Soil carbon dynamics of terrestrial ecosystems play a significant role in the global carbon cycle. Microbial-based decomposition models have seen much growth recently for quantifying this role, yet dormancy as a common strategy used by microorganisms has not usually been represented and tested in these models against field observations. Here we developed an explicit microbial-enzyme decomposition model and examined model performance with and without representation of microbial dormancy at six temperate forest sites of different forest types. We then extrapolated the model to global temperate forest ecosystems to investigate biogeochemical controls on soil heterotrophic respiration and microbial dormancy dynamics at different temporal-spatial scales. The dormancy model consistently produced better match with field-observed heterotrophic soil CO_2 efflux (R_H) than the no dormancy model. Our regional modeling results further indicated that models with dormancy were able to produce more realistic magnitude of microbial biomass (<2% of soil organic carbon) and soil R_H (7.5 ± 2.4 Pg C yr^{1}). Spatial correlation analysis showed that soil organic carbon content was the dominating factor (correlation coefficient = 0.4–0.6) in the simulated spatial pattern of soil R_H with both models. In contrast to strong temporal and local controls of soil temperature and moisture on microbial dormancy, our modeling results showed that soil carbon-to-nitrogen ratio (C:N) was a major regulating factor at regional scales (correlation coefficient = 0.43 to 0.58), indicating scale-dependent biogeochemical controls on microbial dynamics. Our findings suggest that incorporating microbial dormancy could improve the realism of microbial-based decomposition models and enhance the integration of soil experiments and mechanistically based modeling.

Keywords: soil decomposition modeling, microbial dormancy, soil C:N ratio, Michaelis-Menten kinetics

1. Introduction

Soil has always been a focus of climate change studies due to its large carbon (C) stocks – the global soil organic C (SOC) stock is at least four times greater than atmospheric C [*E G Jobbágy and R B Jackson*, 2000] and soil respiration is the second largest flux between the biosphere and the atmosphere following photosynthesis [*J W Raich and C S Potter*, 1995]. Therefore soil C dynamics play a key role in net C sequestration of terrestrial ecosystems and is essential to our understanding of biogeochemical cycles and its climate-C interactions [*IPCC*, 2013].

Since there are limitations of traditional first-order decomposition modeling approach in current earth system models [*K E O Todd-Brown et al.*, 2013], microbial-based soil organic matter decomposition models have been increasingly used in recent studies at both site and global scales [*S D Allison et al.*, 2010; *Y He et al.*, 2014a; *W R Wieder et al.*, 2013]. The current generation of microbial-based decomposition models usually features a common framework where enzyme production and microbial physiology are associated with total microbial biomass (MIC), which has a direct coupling with SOC enzymatic decomposition. A key microbial life-history trait that is usually lacking in these models is microbial dormancy. Dormancy is a common, bet-hedging strategy used by microorganisms when environmental conditions limit growth and reproduction [*S E Jones and J T Lennon*, 2010; *J T Lennon and S E Jones*, 2011]. When microorganisms are confronted with unfavorable conditions, they may enter a reversible state of low metabolic activity and resuscitate when favorable conditions occur. Microorganisms in this state of reduced metabolic activity are not able to drive biogeochemical processes such as soil CO_2 production; therefore only active

75 microorganisms are involved in utilizing substrates in soils [*E Blagodatskaya and Y*
76 *Kuzyakov*, 2013]. Although there are some studies which have explicitly incorporated
77 dormancy into models [*B P Ayati*, 2012; *S Blagodatsky and O Richter*, 1998; *N S Panikov*
78 *and M V Sizova*, 1996; *G Wang et al.*, 2014b; *K W Wirtz*, 2003], they are mostly confined
79 to incubation experiments, and applications of microbial models generally do not
80 consider dormancy.

81 The representation of dormancy in microbial-based decomposition models may be
82 necessary due to several main motivations that led to the inception of this study: (1)
83 current coupled SOC-MIC structure leads to oscillatory behavior of both pools with
84 unrealistically large amplitudes of interannual variation [*Y Wang et al.*, 2013; *W R*
85 *Wieder et al.*, 2013], thus incorporating dormancy may structurally improve model
86 realism; (2) there is a scale mismatch among common measurement procedures of
87 microbial biomass–based physiological metrics. For example, substrate induced
88 respiration and fumigation techniques measure the total microbial biomass when
89 conversion factor 40.04 calculated by [*J Anderson and K Domsch*, 1978] is used, whereas
90 Phospholipid Fatty Acid (PLFA) and fluorescence *in situ* hybridization (FISH) measure
91 the active proportion of total biomass [*E Blagodatskaya and Y Kuzyakov*, 2013; *K Denef*
92 *et al.*, 2009; *C Kramer and G Gleixner*, 2006]; (3) the aforementioned inconsistency may
93 pose challenges in data-model integration and in microbial model comparisons and
94 evaluation; (4) the transition between dormant and active state of microbes can be fast (in
95 the order of hours to days) with substantial magnitude change (e.g., an order of
96 magnitude) in the proportion of active biomass and relative abundance of different
97 phylogenetically clustered microbial groups, but with little changes in total microbial

biomass [*S A Blagodatsky et al.*, 2000; *S B Hagerty et al.*, 2014; *S A Placella et al.*, 2012].

In this study, we hypothesize that: (1) a microbial model incorporated with dormancy would outperform the model without dormancy at site-level parameterization; and (2) a microbial model with dormancy would produce more realistic microbial biomass and soil R_H on both site-level and regional scales. We compared two microbial models that with and without representation of dormancy for site and regional patterns of the modeled SOC and microbial related variables. We also discussed the primary controls on microbial and SOC dynamics at different tempo-spatial scales.

2. Methods

2.1 Model description

Dormancy was incorporated into an existing microbial-enzyme conceptual framework described by Allison et al. [2010], in which an Arrhenius formulation of temperature sensitivity was replaced with a simplified Q_{10} function ($Q_{10}^{\frac{temp-15}{10}}$) to reduce the number of model parameters. The reversible transition between dormant and active state of microbial biomass is assumed to be controlled by environmental cues – directly accessible substrates, as demonstrated in *Wang et al.* [2013]. We integrate *Davidson et al.*'s [2012] conceptual framework of quantifying concentration of soluble C substrates that are directly accessible for microbial assimilation, thus building a direct linkage between environmental factors with microbial state transitions. Substrate quality is also reflected in the model through a generic index of soil C:N ratio [*X Xu et al.*, 2014] and the assimilation of substrate by microorganisms is assumed to be regulated by the C:N ratio of microbial biomass and that of the soil. The model simulates the microbial and

SOC dynamics for the top 30cm of the soil column. The equations for the model with microbial dormancy are as follows:

$$\frac{dSOC}{dt} = Input - \overbrace{V_{\max} Q_{10enz}^{\frac{temp-15}{10}} ENZ \frac{SOC}{K_m + SOC}(120 - CN_{\text{soil}})}^{\text{Decomposition}} \quad (1)$$

$$\frac{dSolubleC}{dt} = Decomposition - \underbrace{\frac{1}{Y_g}\frac{\phi}{\alpha} m_R Q_{10enz}^{\frac{temp-15}{10}} B_a (\frac{CN_{mic}}{CN_{\text{soil}}})^{0.6}}_{\text{Microbial uptake}} + \overbrace{B_a r_{death}}^{\text{Transition from active to dormant}} + \overbrace{ENZr_{loss}}^{\text{Transition from dormant to active}} \quad (2)$$

$$\frac{dB_a}{dt} = (\frac{\phi}{\alpha} - 1) m_R Q_{10mic}^{\frac{temp-15}{10}} B_a (\frac{CN_{mic}}{CN_{soil}})^{0.6} - (1-\phi) m_R Q_{10mic}^{\frac{temp-15}{10}} B_a + \phi m_R Q_{10mic}^{\frac{temp-15}{10}} B_d - B_a r_{prod} - B_a r_{death} \quad (3)$$

$$\frac{dB_d}{dt} = -\beta m_R Q_{10mic}^{\frac{temp-15}{10}} B_d + (1-\phi) m_R Q_{10mic}^{\frac{temp-15}{10}} B_a - \phi m_R Q_{10mic}^{\frac{temp-15}{10}} B_d \quad (4)$$

$$\frac{dENZ}{dt} = B_a r_{prod} - ENZr_{loss} \quad (5)$$

where state variables are SOC, SolubleC, B_a, B_d and ENZ, corresponding to SOC content, SolubleC content, microbial biomass in active and dormant state respectively, and enzyme C (mgC cm^{-2}); temp is soil temperature at each time step t; ϕ is directly accessible substrate for microbial assimilation, calculated based on Michaelis-Menten

kinetics formulated as $\phi = \frac{SolubleC \times D_{liq} \times \theta^3}{K_s + SolubleC \times D_{liq} \times \theta^3}$, D_{liq} is a diffusion coefficient of the substrate in liquid phase (determined by assuming all soluble substrate is directly accessible at the reaction site, $D_{liq} = \frac{1}{(1 - BD / PD)^3}$, BD is bulk density and PD is soil particle density) , θ is volumetric soil moisture content, K_s is corresponding Michaelis constant [*E A Davidson et al.*, 2012]. Detailed description for other parameters is summarized in Table 1. Adding up the equation 3 and 4 shown above gives the model without dormancy.

Environmental factors such as substrate availability are often thought to be a direct control of the transition between active and dormant states of microorganisms [*J T Lennon and S E Jones*, 2011]. Therefore we adopted the formulation described in Wang *et al.*, [2014a], where the transition between active and dormant state of microorganisms is scaled linearly with substrate availability and the direction of the net transition is determined by the balance of maintenance metabolic requirement and substrate availability.

We recognize that our model only simulates C dynamics, and decomposition is effectively influenced by various nutrients through kinetic and stoichiometric constrains that are not explicitly represented in this model [*S D Allison*, 2005; *S E Hobbie et al.*, 2002; *R L Sinsabaugh et al.*, 2013; *K-J van Groenigen et al.*, 2006]. Instead of using a more sophisticated modeling framework, we introduced a temperature and population size dependent scaling factor on the potential microbial death rate, formulated as $1.5^{\frac{temp-15}{10}} \times \frac{B_a}{SOC \times 0.025}$, where a metabolic temperature sensitivity of 1.5 and a

158 population capacity of 2.5% of SOC is assumed for temperate forest soils [*X Xu et al.*,
159 2013; *G Yvon-Durocher et al.*, 2012]. This multiplier is used to modify the parameter
160 r_{death} and implicitly represents competition for nutrients and down regulates microbial
161 growth.

162 **2.2 Model calibration and validation**

163 We calibrated the model at 6 different temperate forest sites in northeastern China
164 (3) and conterminous USA (3) with a latitudinal span of 38 – 45°N using a global
165 optimization algorithm known as the SCE-UA (shuffled complex evolution; [*Q Duan et*
166 *al.*, 1992; *Q Duan et al.*, 1994] (Table 2). The 3 northeastern China sites were all
167 trenched plots with monthly measured R_H, soil temperature and gravimetric soil moisture
168 content at 10cm from 2004 to 2007 [*C Wang and J Yang*, 2007; *C Wang et al.*, 2006].
169 The 3 US sites are part of the AmeriFlux network. The level 2 (gap-filled) eddy
170 covariance data with half-hourly measured soil temperature (at 10cm, °C), volumetric soil
171 moisture content (at 10cm, %; VSM) and automated soil chamber measured soil
172 respiration (umol m^{-2} s^{-1}) were used for this study [*L Gu et al.*, 2006; *J Irvine and B E*
173 *Law*, 2002]. Approximately 50% of soil respiration was assumed to be R_H [*P J Hanson et*
174 *al.*, 2000]. Litterfall was assumed to be a fixed proportion (0.3) of net primary production
175 (NPP), and we assume NPP/GPP = 0.45 (gross primary production, GPP) [*B E Law et al.*,
176 2001; *B E Law et al.*, 2003]. GPP at US-Me2 and US-MRf sites (see Table 2) were also
177 obtained from level 2 data, but were not available for US-MOz site. Therefore for the R_H
178 measurement period (2004-2007), we used level 4 gap-filled net ecosystem exchange
179 (NEE) and we calculated GPP based on NEE and meteorological data using an online
180 flux partitioning tool (http://www.bgc-jena.mpg.de/~MDIwork/ eddyproc/upload.php) [*G*

181 *Lasslop et al.*, 2010]. Site level state variables (e.g. SOC content) served as initial states
182 for the model calibration. Note that we rescaled the prior used in inverse modeling for
183 parameters on per unit of microbial biomass basis (Table 1). The first 75% of total
184 available data at each site was used for calibration and the remaining was used for
185 validation. Model evaluation statistics were calculated using the whole data series.

186 **2.3 Data sources for spatial extrapolation**

187 We used the above calibrated ecosystem specific parameters and extrapolated to
188 the whole temperate forest region defined as the latitudinal band from 25°N to 50° N. We
189 did not include the Southern Hemisphere due to limited forest coverage and lack of
190 calibration site located in the region. The average parameters of the corresponding forest
191 types are used for each forest type involved the latitudinal band. Forest land cover
192 information was extracted from Moderate Resolution Imaging Spectroradiometer
193 (MODIS) land cover product (MCD12C1) for the period 2000-2012 and annual mean
194 land cover distribution was used. The original 0.05°×0.05° (lon×lat) resolution grid was
195 aggregated to 0.5°×0.5° using a majority resampling approach to best preserve the spatial
196 structure of the major classes. NPP (2000-2012, annual mean) data were extracted from
197 MOD17A3 L4 Global 1km product (Version-55) [*M Zhao and S W Running*, 2010]. The
198 original data were aggregated to 0.5°×0.5° using the areal mean. Soil physical properties
199 and organic C and N content of the top 30cm were obtained from gridded Global Soil
200 Dataset for use in Earth System Models (GSDE) dataset [*W Shangguan et al.*, 2014].
201 Particle density was calculated based on bulk density and porosity, and porosity was
202 estimated using VSM at -10kPa (provided in GSDE). Specifically, we assumed saturated
203 VSM as same as VSM at -10kPa for silt loam soil and we added 10% for sand loam soil

based on the soil water retention curve [*W M Cornelis et al.*, 2005]. Soil was classified according to soil taxonomy [Soil Survey Staff, 2003] and using sand, silt, and clay content from GSDE data set. For transient simulations, we used CMIP5 historical runs initialized in year 2006 from CCSM4 land modeling realm (r1i1p1) to retrieve soil temperature (tsl, average of top 10cm) and soil water content in the top 10cm (mrsos) (http://www.earthsystemgrid.org). Soil water content in mass was converted to soil volumetric moisture using relevant soil properties provided by GSDE dataset. Soil temperature and moisture data were interpolated from 0.9 × 1.25 to 0.5 × 0.5 using bilinear interpolation method [*T Wang et al.*, 2006].

2.4 Statistical Analysis

Because we are interested in the overall functional correlations between dormancy and related environmental factors, we choose to use simple Pearson correlation for spatial correlation analysis. The spatial extrapolation used the soil temperature and moisture profile from 2006 and ran for 3 years, and the simulation results for the last year was used for spatial grid-based and temporal correlation analysis.

3. Results

3.1 Site level calibration and validation

Both the dormancy and no-dormancy models can reproduce the observed soil R_H reasonably well. The adj-R^2 of the dormancy model ranges from 0.51 to 0.76 (Table 3), and four out of the six sites had positive Nash-Sutcliffe model efficiency coefficients (0.43 to 0.75). The no-dormancy model performed slightly worse, as adj-R^2 ranged from 0.36 to 0.73; the Nash coefficients were also slightly lower (Table 3). The no-dormancy model did not adequately reproduce the observed soil respiration well at Missouri Ozark

AmeriFlux site (US-MOz) (adj-R^2 = 0.32), likely because the high SOC content at this site makes it more difficult to find an appropriate K_m due to its high sensitivity (see discussion in Section 4.3). A paired t-test on adj-R^2 showed marginally significant difference between the two models (df=5, p=0.098). Simulated dynamics of various C pools (e.g., SOC, SolubleC, ENZ and MIC) of the two models exhibited similar patterns over time (Figure 1, 2). SOC at US-Me2 showed a slight decline over the course of 11 years in both models (Figure 1a,e), with SolubleC content showing a seasonal fluctuation anti-phased with microbial biomass due to active substrate uptake during summer thus less substrate availability, and suppressed microbial activity during winter, which led to the accumulation of substrate (Figure 1a,e). The active proportion of microbial biomass tracked the changes in soil moisture tightly, despite the opposite moisture regimes at the two sites where US-Me2 experienced moderate drought during summer while CN-Lar featured benign moisture conditions for microbial decomposition (Figure 1b,f; Figure 2 b,f). It is worth noting here that the seasonal MIC amplitude (calculated as the difference between annual maximum and minimum MIC) was always much larger (up to two times larger) in no-dormancy models than in the dormancy models (Table 3; Figure 1b,g; Figure 2b,g), and there was significant difference between the two models (df=5, p=0.033). Thus, the magnitude of the oscillations in the dormancy model is significantly smaller than in the no-dormancy model.

3.2 Inversed model parameters

Parameters that have biophysical meaning should reflect the patterns that characterize different ecosystem properties. Our mixed forest (CN-fixed) generally showed intermediate parameter values compared to deciduous broadleaf and evergreen

needleleaf forests (Figure 3). Some parameters exhibited distinct patterns among deciduous broadleaf and evergreen needleleaf forests. For instance, microbial maintenance respiration (mR) was overall higher in evergreen needleleaf forests than deciduous broadleaf forests (Figure 3c), but the opposite was seen for initial active fraction (Figure 3l), indicating more stressed soil environment and higher energy limitation for microorganisms in evergreen needleleaf forests due to less substrate availability and poorer substrate quality. For other parameters, especially microbial and enzyme related parameters, the differences between the two major forest types were not significant (Figure 3f-i). Km is highest in US-MOz (Figure 3e), because it has the highest SOC content and the Michaelis-Menten formulation makes high Km important for maintaining the relative substrate level in a reasonable range, which suggests the high sensitivity of the half-saturation constant to SOC in the Michaelis-Menten formulation.

3.3 Spatial Extrapolation

3.3.1 Spatial distribution of soil R_H and microbial biomass

The two models both simulated soil R_H ranging between 300 and 1000 gC m^{-2} yr^{-1}. The spatial pattern of the soil R_H of the dormancy and no-dormancy model differed in large areas of northwestern and southeastern US and in southern China, with no-dormancy model simulating about 30% higher respiration than that of the dormancy model (Figure 4a,b). The soil R_H of other regions was generally comparable between the two models. The total soil R_H of all temperate forests from the dormancy model amounted to 6.88 PgC yr^{-1}, and 7.99 PgC yr^{-1} from no-dormancy model. While there may not be significant difference in the simulated spatial soil R_H between the models, the MIC/SOC ratio showed distinct patterns in both magnitude and spatial distribution of the

two models (Figure 4c,d). Here the MIC is the total microbial biomass including active and dormant microbes for dormancy model. The no-dormancy model overall simulated about two-times higher MIC/SOC ratio for temperate forests, especially in northeastern US, south Europe, and Japan, than the dormancy model. In the no-dormancy model, the MIC/SOC ratio can reach about 4% (Figure 4d) whereas in the dormancy model the ratio ranged from 0.5% to 2% (Figure 4c). Our simulated spatial soil R_H of temperate forests was high at the Great lakes regions in the US where SOC content was also reported high from the GSDE dataset (Figure 4a,b). Grid cell based spatial correlation analysis showed that in both models, soil R_H was negatively affected by bulk density and particle density ($\rho \approx -0.36$ and -0.48, respectively, $P<0.001$), but had a significant correlation with soil C:N ratio ($\rho \approx 0.3$, $P<0.001$) and especially organic matter content ($\rho \approx 0.89$, $P<0.001$)(Table 4). Soil temperature and moisture also had significant positive effects on soil R_H ($\rho \approx 0.17$ and 0.14, respectively, $P<0.001$), but was not as strong as the SOC.

3.3.2 Spatial pattern of microbial dormancy and its controlling factors

Annual active proportion of microbial biomass ranged from 2% to 40% across temperate forests (Figure 5a,b). The spatial distribution of active fraction was relatively the same across seasons. Seasonal active proportion of microbial biomass in summer was generally about 10% higher than in winter for large areas of northeastern US and northeaster China, whereas northwestern US, Europe and southern China featured relatively constant active fraction across seasons (Figure 5a,b). Grid cell based spatial correlation analysis showed that the soil C:N ratio was a major controlling factor on dormancy ($\rho=0.41$ in summer and 0.21 in winter , respectively, $P<0.001$, Table 4), indicating higher substrate availability (higher C:N ratio), lower dormancy proportion

296 (higher active fraction). Annual temperature and moisture were weak controls on spatial
297 dormancy pattern ($\rho<0.1$) except that winter active fraction had a stronger positive
298 correlation with annual temperature ($\rho=0.17$, $P<0.001$). However, temperature and
299 moisture had very strong local controls on dormancy on temporal scales, with moisture
300 had mostly strong positive temporal correlations with active fraction ($\rho>0.8$, Figure 6a),
301 as moisture was formulated to directly control substrate availability. Temperature showed
302 negative temporal correlation with active fraction ($\rho<-0.5$, Figure 6b), primarily due to
303 the negative covariation between temperature and moisture in the CCSM4 results (Figure
304 6c). It is worth noting here that, although annual temperature and moisture had weak
305 controls on spatial patterns of active fraction, the seasonal amplitude of soil temperature
306 and moisture generally exhibited higher correlations with active fraction ($\rho>0.1$ and
307 $P<0.001$ for summer and winter, Table 4), suggesting there is a high sensitivity of active-
308 dormancy transition to seasonal changes in moisture levels on spatial scales.

309 **4. Discussion**

310 **4.1 Model performance and limitations**

311 A synthesis by *Bond-Lamberty et al.* [2004] documented soil R_H from
312 temperate forests to range from 300 to 800 gC m^{-2} yr^{-1}. We calculated the regional total
313 soil R_H based on reported mean value of 600 gC m^{-2} yr^{-1} and the land cover map used in
314 this study and resulted in total soil R_H to be around 7.11 PgC yr^{-1}. The dormancy model
315 thus produced closer estimates to this synthetic estimate with 6.88 PgC yr^{-1}, whereas the
316 no-dormancy model overestimated soil R_H of 7.99 PgC yr^{-1}. Despite the comparable
317 results between our simulated soil R_H and synthesized observations, we used a simplified
318 modeling framework without explicitly considering other key element cycles. Although

319 we used soil C:N ratio to indicate substrate quality and its effects on microbial
320 assimilation as a representative index, the coupled dynamics of kinetics and
321 stoichiometric constrains on microbial physiology, which also pose key controls on
322 decomposition dynamics, are not incorporated [*S D Allison*, 2005; *R L Sinsabaugh et al.*,
323 2013; *K-J van Groenigen et al.*, 2006]. While the simplified framework may be sufficient
324 to serve the purpose of this study, a more complex modeling scheme that accounts for the
325 stoichiometry of other key elements should be able to reveal more biogeochemical
326 controls which can then be benchmarked with observations to improve model
327 performance.

328 **4.2 Implications for informing experimental needs**

329 Rainfall induced activation of dormant biomass can generate soil CO_2 pulses
330 comparable in magnitude to the annual net C exchange of many terrestrial ecosystems,
331 such as Mediterranean [*S A Placella et al.*, 2012; *L Xu et al.*, 2004]. Particularly, such
332 drying-rewetting events can exert stress on soil microbial communities and cause
333 decrease in soil basal respiration while total biomass increases [*N Fierer and J P Schimel*,
334 2002]. In addition, changes in soil temperature and moisture conditions can induce
335 responses in microbial basal respiration that were not explained by changes in total
336 microbial biomass but rather changes in the physiology of soil microbial communities
337 such as resuscitation of physiologically clustered microbial groups [*S B Hagerty et al.*,
338 2014; *S A Placella et al.*, 2012; *J M Steinweg et al.*, 2012; *V Suseela et al.*, 2012]. In
339 contrast to seasonal variation in soil R_H driven by changes in temperature and moisture in
340 a variety of ecosystems [*V Suseela and J S Dukes*, 2012; *V Suseela et al.*, 2012], total
341 microbial biomass is generally unaffected by seasonality [*E Blume et al.*, 2002; *N*

342 *Gunapala and K Scow*, 1998]. All of these indicate that soil respiration responses to
343 environmental conditions are more closely associated with active portion of microbial
344 biomass than the total. Thus, the no-dormancy model that does not distinguish microbial
345 biomass with different physiological states may not correctly represent the microbe-soil
346 interactions. Similarly, using total biomass as an important metric in both experiments
347 and modeling may also hinder effective data-model integration.

348 Our modeling results demonstrate that the ecosystem level controls (substrate
349 quality and availability) on the average dormancy level (active proportion) at large spatial
350 scales are different from that at local transient scales (temporal effects of soil moisture).
351 This suggests that both site-level and spatial data should be used for model validation,
352 because it is usually easier for model to reproduce site-level, short-term observations with
353 data assimilation techniques, but much more difficult to capture spatial patterns [*K E O*
354 *Todd-Brown et al.*, 2013] and long-term dynamics [*He et al.,* 2014b]. In this study, we
355 successfully reproduced soil R_H at six temperature forest sites, but our extrapolated soil
356 R_H revealed the potential issues with applying Michaelis-Menten kinetics on ecosystem
357 scales and yielded high soil R_H in the northeastern US due to the high SOC content in
358 that region. Such insufficiency in the model structure may not be disclosed at site-level
359 examination. Therefore, spatially gridded comprehensive soil C and microbial physiology
360 metrics would be tremendously helpful in model validation and assessment. For example,
361 the contrasting controls of bulk density, particle density and organic C content on
362 simulated soil R_H likely reflects covariation among these variables, because with
363 increasing particle density C concentration decreased, implying that the soil organic

matter accumulations were thinner [*P Sollins et al.*, 2009]. Our simulated soil R_H is then able to reflect the spatial controls of soil physical properties on decomposition.

Uncertainty in driving data for decomposition models may also be substantial and experimental measurements on large spatial scales would also be helpful. For example, the CCSM4 simulation we used cannot reproduce the surface frozen soil in northeastern China we observed in the site level measurements (Figure 2f), which potentially could introduce inaccuracies in model results. Note that in southern China broadleaf temperate forest does not show high temporal positive correlation of active proportion with soil moisture, this is likely because soil moisture is relatively constant throughout the year [*X Tang et al.*, 2006], thus soil moisture may not be the primary limiting factor on dormancy-active transition in that region. More experimental data in that region should help benchmark both simulated soil moisture and temperature.

4.3 Implications for informing future model development

The high correlation between soil R_H and the organic C content in the top 30cm (Table 4) in our analysis may be attributable to the Michaelis-Menten kinetics we used in the SOC enzymatic decay process (Eqn 1), where SOC content directly controls saturation level of the organic matter. Such high positive correlation between soil R_H and the organic C content were not reported for other formulations (e.g., first-order kinetics in CMIP5 simulations where turnover time and net primary production are both positively correlated with SOC content across different earth system models) where decomposition rate is also associated with SOC content [*K E O Todd-Brown et al.*, 2013]. Thus we argue that Michaelis-Menten kinetics may not be suitable for characterizing SOC enzymatic decay process when different soil layers are treated as one unified substrate. This is

because that Michaelis-Menten kinetics has an implicit assumption that all substrate are accessible to enzymes under a homogeneous spatial distribution, and that a solution environment where Michaelis-Menten kinetics was usually applied to is a good example that demonstrates the homogeneity requirement [*L Michaelis and M L Menten*, 1913], thus Michaelis-Menten kinetics has a spatial constrain on relatively local scales. In addition, Michaelis-Menten formulation is derived under the assumption that enzymatic kinetics can cause a significant change on substrate levels [*L Michaelis and M L Menten*, 1913], which is unrealistic for the microbial extracellular hydrolysis of SOC due to soil mineral-organic matter interaction and occlusion of SOC in soil aggregates which forms physical barriers [*B P Ayati*, 2012; *N S Panikov and M V Sizova*, 1996]. These limitations may explain the under-performance of the no-dormancy model at US-MOz site which has the highest SOC content among 6 sites. Although this issue is less notable in dormancy model, its unrealistic spatial distribution of high soil R_H in high SOC regions still suggests some issues of using Michaelis-Menten kinetics when treating a large SOC as homogeneous (Table 4). We propose that a better representation of soil vertical heterogeneity (e.g., [*C Koven et al.*, 2013]) would be essential to using Michaelis-Menten kinetics in microbial-based decomposition models . Large SOC content likely induced mismatch of the temporal scale of SOC change with that of microbial activity. To reconcile the homogeneity assumption of Michaelis-Menten dynamics and the localization of actual SOC enzymatic decay, vertical heterogeneity can be implemented using multi-layer soil model structure or depth-resolved SOC profile thus ensuring certain degree of homogeneity of SOC and enzyme distribution at each depth increment [*Y He et al.*, 2014b]. Stabilization of organic matter by interaction with poorly crystalline

410 minerals is also a key mechanisms missing in current models [*B P Ayati*, 2012; *N S*
411 *Panikov and M V Sizova*, 1996] and should be incorporated in future model development.
412 In both models, soil temperature and moisture exhibited similar levels of controls
413 on soil R_H (Table 4), this is likely attributed to the way soil moisture effect is defined in
414 the model where it directly controls substrate availability. Such formulation with direct
415 coupling with microbial activity can shed light on improving soil moisture representation
416 in decomposition models as current first-order formulation in decomposition models only
417 yield in marginal effects of soil moisture [*K E O Todd-Brown et al.*, 2013].
418 **5. Conclusion**
419 Microbial life-history traits such as dormancy play an important role in
420 biogeochemical cycles. It has been widely observed that the active portion of microbial
421 biomass, rather than the total biomass, explains the changes in microbial basal respiration
422 rates. This study examines whether including dormancy in microbial-based soil
423 decomposition model can improve the estimates of SOC dynamics and other microbial
424 related metrics. Our results showed that although both dormancy and no-dormancy
425 models can capture the field observed soil R_H, the no-dormancy model exhibited larger
426 seasonal oscillation and overestimation in microbial biomass. Our regional modeling
427 results also indicated that models with dormancy were able to produce more realistic
428 magnitude in microbial biomass and soil R_H, and that Michaelis-Menten kinetics may not
429 be appropriate for models that do not vertically resolve decomposition dynamics in the
430 soil profile. This study also identified the scale-dependent biogeochemical controls on
431 microbial dynamics. Overall, our findings suggest future microbial model development
432 should consider the representation of microbial dormancy, which will both improve the

433 realism of microbial-based decomposition models and enhance the avenues for
434 integration of empirical soil experiments and modeling.

Acknowledgement

We would like to thank Xiaofeng Xu for his suggestions on an earlier version of this manuscript, and Yang Bai for his help with partitioning related AmeriFlux data. We also would like to thank AmefiFlxu PIs for making these long term observations publicly available. This research is supported with NSF projects (DEB-#0919331; NSF-0630319 to Q.Z.), the NASA Land Use and Land Cover Change program (NASA-NNX09AI26G to Q.Z.), Department of Energy (DE-FG02-08ER64599 to Q.Z.), and the NSF Division of Information & Intelligent Systems (NSF-1028291 to Q.Z.). Data from analyses and figures will be archived to the Purdue University Research Repository and can be accessed by contacting the corresponding author (Y.H.).

446 **References:**

447 Soil Survey Staff, 2003. Keys to soil taxonomy. 9th ed. USDA, Washington, DC.
448 Michaelis, L. and Menten, M. L.: The kenetics of the inversion effect, Biochem. Z., 49,
449 333–369, 1913.
450 Allison, S. D. (2005), Cheaters, diffusion and nutrients constrain decomposition by
451 microbial enzymes in spatially structured environments, *Ecology Letters*, *8*(6),
452 626-635.
453 Allison, S. D., M. D. Wallenstein, and M. A. Bradford (2010), Soil-carbon response to
454 warming dependent on microbial physiology, *Nature Geoscience*, *3*(5), 336-340.
455 Anderson, J., and K. Domsch (1978), A physiological method for the quantitative
456 measurement of microbial biomass in soils, *Soil Biology and Biochemistry*, *10*(3),
457 215-221.
458 Ayati, B. P. (2012), Microbial dormancy in batch cultures as a function of substrate-
459 dependent mortality, *Journal of theoretical biology*, *293*, 34-40.
460 Blagodatskaya, E., and Y. Kuzyakov (2013), Active microorganisms in soil: critical
461 review of estimation criteria and approaches, *Soil Biology and Biochemistry*, *67*,
462 192-211.
463 Blagodatsky, S., and O. Richter (1998), Microbial growth in soil and nitrogen turnover: a
464 theoretical model considering the activity state of microorganisms, *Soil Biology*
465 *and Biochemistry*, *30*(13), 1743-1755.
466 Blagodatsky, S. A., O. Heinemeyer, and J. Richter (2000), Estimating the active and total
467 soil microbial biomass by kinetic respiration analysis, *Biology and fertility of*
468 *soils*, *32*(1), 73-81.
469 Blume, E., M. Bischoff, J. Reichert, T. Moorman, A. Konopka, and R. Turco (2002),
470 Surface and subsurface microbial biomass, community structure and metabolic
471 activity as a function of soil depth and season, *Applied Soil Ecology*, *20*(3), 171-
472 181.
473 Bond-Lamberty, B., C. Wang, and S. T. Gower (2004), A global relationship between the
474 heterotrophic and autotrophic components of soil respiration?, *Global Change*
475 *Biology*, *10*(10), 1756-1766.
476 Cornelis, W. M., M. Khlosi, R. Hartmann, M. Van Meirvenne, and B. De Vos (2005),
477 Comparison of unimodal analytical expressions for the soil-water retention curve,
478 *Soil Science Society of America Journal*, *69*(6), 1902-1911.
479 Davidson, E. A., S. Samanta, S. S. Caramori, and K. Savage (2012), The Dual Arrhenius
480 and Michaelis–Menten kinetics model for decomposition of soil organic matter at
481 hourly to seasonal time scales, *Global Change Biology*, *18*(1), 371-384.
482 Denef, K., D. Roobroeck, M. C. Manimel Wadu, P. Lootens, and P. Boeckx (2009),
483 Microbial community composition and rhizodeposit-carbon assimilation in
484 differently managed temperate grassland soils, *Soil Biology and Biochemistry*,
485 *41*(1), 144-153.
486 Duan, Q., S. Sorooshian, and V. Gupta (1992), Effective and efficient global optimization
487 for conceptual rainfall-runoff models, *Water Resources Research*, *28*(4), 1015-
488 1031.
489 Duan, Q., S. Sorooshian, and V. K. Gupta (1994), Optimal use of the SCE-UA global
490 optimization method for calibrating watershed models, *Journal of Hydrology*,
491 *158*(3–4), 265-284.

Fierer, N., and J. P. Schimel (2002), Effects of drying–rewetting frequency on soil carbon and nitrogen transformations, *Soil Biology and Biochemistry*, *34*(6), 777-787.

Fu, M., C. Wang, Y. Wang, and S. Liu (2009), Temporal and spatial patterns of soil nitrogen mineralization and nitrification in four temperate forests, *Acta Ecologica Sinica*, *29*(7), 3747-3758.

German, D. P., K. R. Marcelo, M. M. Stone, and S. D. Allison (2012), The Michaelis–Menten kinetics of soil extracellular enzymes in response to temperature: a cross-latitudinal study, *Global Change Biology*, *18*(4), 1468-1479.

Gu, L., T. Meyers, S. G. Pallardy, P. J. Hanson, B. Yang, M. Heuer, K. P. Hosman, J. S. Riggs, D. Sluss, and S. D. Wullschleger (2006), Direct and indirect effects of atmospheric conditions and soil moisture on surface energy partitioning revealed by a prolonged drought at a temperate forest site, *Journal of Geophysical Research: Atmospheres*, *111*(D16), D16102.

Gunapala, N., and K. Scow (1998), Dynamics of soil microbial biomass and activity in conventional and organic farming systems, *Soil Biology and Biochemistry*, *30*(6), 805-816.

Hagerty, S. B., K. J. van Groenigen, S. D. Allison, B. A. Hungate, E. Schwartz, G. W. Koch, R. K. Kolka, and P. Dijkstra (2014), Accelerated microbial turnover but constant growth efficiency with warming in soil, *Nature Climate Change*, *4*(10), 903-906.

Hanson, P. J., N. T. Edwards, C. T. Garten, and J. A. Andrews (2000), Separating root and soil microbial contributions to soil respiration: A review of methods and observations, *Biogeochemistry*, *48*(1), 115-146.

He, Y., J. Yang, Q. Zhuang, A. D. McGuire, Q. Zhu, Y. Liu, and R. O. Teskey (2014a), Uncertainty in the fate of soil organic carbon: A comparison of three conceptually different decomposition models at a larch plantation, *Journal of Geophysical Research: Biogeosciences*, *119*(9), 2014JG002701.

He, Y., Q. Zhuang, J. W. Harden, A. D. McGuire, Z. Fan, Y. Liu, and K. P. Wickland (2014b), The implications of microbial and substrate limitation for the fates of carbon in different organic soil horizon types of boreal forest ecosystems: a mechanistically based model analysis, *Biogeosciences*, *11*(16), 4477-4491.

Hobbie, S. E., K. J. Nadelhoffer, and P. Hogberg (2002), A synthesis: The role of nutrients as constraints on carbon balances in boreal and arctic regions, *Plant and Soil*, *242*(1), 163-170.

IPCC (2013), Summary for Policymakers. In: Climate Change 2013: The Physical Science Basis. Contribution of Working Group I to the Fifth Assessment Report of the Intergovernmental Panel on Climate Change*Rep.*, Cambridge, United Kingdom and New York, NY, USA.

Irvine, J., and B. E. Law (2002), Contrasting soil respiration in young and old-growth ponderosa pine forests, *Global Change Biology*, *8*(12), 1183-1194.

Jobbágy, E. G., and R. B. Jackson (2000), The vertical distribution of soil organic carbon and its relation to climate and vegetation, *Ecological Applications*, *10*(2), 423-436.

Jones, S. E., and J. T. Lennon (2010), Dormancy contributes to the maintenance of microbial diversity, *Proceedings of the National Academy of Sciences*, *107*(13), 5881-5886.

Koven, C., W. Riley, Z. Subin, J. Tang, M. Torn, W. Collins, G. Bonan, D. Lawrence, and S. Swenson (2013), The effect of vertically resolved soil biogeochemistry and alternate soil C and N models on C dynamics of CLM4, *Biogeosciences*, *10*, 7109-7131.

Kramer, C., and G. Gleixner (2006), Variable use of plant-and soil-derived carbon by microorganisms in agricultural soils, *Soil Biology and Biochemistry*, *38*(11), 3267-3278.

Lasslop, G., M. Reichstein, D. Papale, A. D. Richardson, A. Arneth, A. Barr, P. Stoy, and G. Wohlfahrt (2010), Separation of net ecosystem exchange into assimilation and respiration using a light response curve approach: critical issues and global evaluation, *Global Change Biology*, *16*(1), 187-208.

Law, B. E., P. E. Thornton, J. Irvine, P. M. Anthoni, and S. Van Tuyl (2001), Carbon storage and fluxes in ponderosa pine forests at different developmental stages, *Global Change Biology*, *7*(7), 755-777.

Law, B. E., O. J. Sun, J. Campbell, S. Van Tuyl, and P. E. Thornton (2003), Changes in carbon storage and fluxes in a chronosequence of ponderosa pine, *Global Change Biology*, *9*(4), 510-524.

Lennon, J. T., and S. E. Jones (2011), Microbial seed banks: the ecological and evolutionary implications of dormancy, *Nature Reviews Microbiology*, *9*(2), 119-130.

Liu, S., and C. Wang (2010), Spatio-temporal patterns of soil microbial biomass carbon and nitrogen in five temperate forest ecosystems, *Acta Ecologica Sinica*, *30*(12), 3135-3143.

Michaelis, L., and M. L. Menten (1913), The kenetics of the inversion effect, *Biochemische Zeitschrift*, *49*, 333-369.

Panikov, N. S., and M. V. Sizova (1996), A kinetic method for estimating the biomass of microbial functional groups in soil, *Journal of Microbiological Methods*, *24*(3), 219-230.

Placella, S. A., E. L. Brodie, and M. K. Firestone (2012), Rainfall-induced carbon dioxide pulses result from sequential resuscitation of phylogenetically clustered microbial groups, *Proceedings of the National Academy of Sciences*, *109*(27), 10931-10936.

Purich, D. L. (2009), *Contemporary Enzyme Kinetics and Mechanism: Reliable Lab Solutions*, Academic Press.

Raich, J. W., and C. S. Potter (1995), Global Patterns of carbon-dioxide emissions from soils, *Global Biogeochemical Cycles*, *9*(1), 23-36.

Schimel, J. P., and M. N. Weintraub (2003), The implications of exoenzyme activity on microbial carbon and nitrogen limitation in soil: a theoretical model, *Soil Biology and Biochemistry*, *35*(4), 549-563.

Shangguan, W., Y. Dai, Q. Duan, B. Liu, and H. Yuan (2014), A global soil data set for earth system modeling, *Journal of Advances in Modeling Earth Systems*, *6*(1), 249-263.

Sinsabaugh, R. L., S. Manzoni, D. L. Moorhead, and A. Richter (2013), Carbon use efficiency of microbial communities: stoichiometry, methodology and modelling, *Ecology Letters*, *16*(7), 930-939.

583 Sollins, P., M. Kramer, C. Swanston, K. Lajtha, T. Filley, A. Aufdenkampe, R. Wagai,
584 and R. Bowden (2009), Sequential density fractionation across soils of contrasting
585 mineralogy: evidence for both microbial- and mineral-controlled soil organic
586 matter stabilization, *Biogeochemistry*, *96*(1-3), 209-231.
587 Steinweg, J. M., J. S. Dukes, and M. D. Wallenstein (2012), Modeling the effects of
588 temperature and moisture on soil enzyme activity: Linking laboratory assays to
589 continuous field data, *Soil Biology and Biochemistry*, *55*(0), 85-92.
590 Suseela, V., and J. S. Dukes (2012), The responses of soil and rhizosphere respiration to
591 simulated climatic changes vary by season, *Ecology*.
592 Suseela, V., R. T. Conant, M. D. Wallenstein, and J. S. Dukes (2012), Effects of soil
593 moisture on the temperature sensitivity of heterotrophic respiration vary
594 seasonally in an old-field climate change experiment, *Global Change Biology*,
595 *18*(1), 336-348.
596 Tang, X., S. Liu, G. Zhou, D. Zhang, and C. Zhou (2006), Soil-atmospheric exchange of
597 CO2, CH4, and N2O in three subtropical forest ecosystems in southern China,
598 *Global Change Biology*, *12*(3), 546-560.
599 Thomas, C. K., B. E. Law, J. Irvine, J. G. Martin, J. C. Pettijohn, and K. J. Davis (2009),
600 Seasonal hydrology explains interannual and seasonal variation in carbon and
601 water exchange in a semiarid mature ponderosa pine forest in central Oregon,
602 *Journal of Geophysical Research: Biogeosciences*, *114*(G4), G04006.
603 Todd-Brown, K. E. O., J. T. Randerson, W. M. Post, F. M. Hoffman, C. Tarnocai, E. A.
604 G. Schuur, and S. D. Allison (2013), Causes of variation in soil carbon
605 simulations from CMIP5 Earth system models and comparison with observations,
606 *Biogeosciences*, *10*(3), 1717-1736.
607 van Groenigen, K.-J., J. Six, B. A. Hungate, M.-A. de Graaff, N. van Breemen, and C.
608 van Kessel (2006), Element interactions limit soil carbon storage, *Proceedings of*
609 *the National Academy of Sciences*, *103*(17), 6571-6574.
610 Wang, C., and J. Yang (2007), Rhizospheric and heterotrophic components of soil
611 respiration in six Chinese temperate forests, *Global Change Biology*, *13*(1), 123-
612 131.
613 Wang, C., J. Yang, and Q. Zhang (2006), Soil respiration in six temperate forests in
614 China, *Global Change Biology*, *12*(11), 2103-2114.
615 Wang, G., M. A. Mayes, L. Gu, and C. W. Schadt (2013), Representation of Dormant and
616 Active Microbial Dynamics for Ecosystem Modeling, *arXiv preprint*
617 *arXiv:1309.2617*.
618 Wang, G., M. A. Mayes, L. Gu, and C. W. Schadt (2014a), Representation of Dormant
619 and Active Microbial Dynamics for Ecosystem Modeling, *PLoS ONE*, *9*(2),
620 e89252.
621 Wang, G., S. Jagadamma, M. A. Mayes, C. W. Schadt, J. M. Steinweg, L. Gu, and W. M.
622 Post (2014b), Microbial dormancy improves development and experimental
623 validation of ecosystem model, *The ISME journal*.
624 Wang, T., A. Hamann, D. Spittlehouse, and S. Aitken (2006), Development of scale-free
625 climate data for Western Canada for use in resource management, *International*
626 *journal of climatology*, *26*(3), 383-397.
627 Wang, Y., B. Chen, W. Wieder, Y. Luo, M. Leite, B. Medlyn, M. Rasmussen, M. Smith,
628 F. Agusto, and F. Hoffman (2013), Oscillatory behavior of two nonlinear

629 microbial models of soil carbon decomposition, *Biogeosciences Discussions*,
630 *10*(12), 19661-19700.
631 Wieder, W. R., G. B. Bonan, and S. D. Allison (2013), Global soil carbon projections are
632 improved by modelling microbial processes, *Nature Climate Change*, *3*(10), 909-
633 912.
634 Wirtz, K. W. (2003), Control of biogeochemical cycling by mobility and metabolic
635 strategies of microbes in the sediments: an integrated model study, *FEMS*
636 *Microbiology Ecology*, *46*(3), 295-306.
637 Xu, L., D. D. Baldocchi, and J. Tang (2004), How soil moisture, rain pulses, and growth
638 alter the response of ecosystem respiration to temperature, *Global*
639 *Biogeochemical Cycles*, *18*(4).
640 Xu, X., P. E. Thornton, and W. M. Post (2013), A global analysis of soil microbial
641 biomass carbon, nitrogen and phosphorus in terrestrial ecosystems, *Global*
642 *Ecology and Biogeography*, n/a-n/a.
643 Xu, X., J. P. Schimel, P. E. Thornton, X. Song, F. Yuan, and S. Goswami (2014),
644 Substrate and environmental controls on microbial assimilation of soil organic
645 carbon: a framework for Earth system models, *Ecology Letters*, n/a-n/a.
646 Yang, J., and C. Wang (2005), Soil carbon storage and flux of temperate forest
647 ecosystems in northeastern China, *Acta Ecologica Sinica*, *25*(11), 2875-2882.
648 Yvon-Durocher, G., J. M. Caffrey, A. Cescatti, M. Dossena, P. del Giorgio, J. M. Gasol,
649 J. M. Montoya, J. Pumpanen, P. A. Staehr, and M. Trimmer (2012), Reconciling
650 the temperature dependence of respiration across timescales and ecosystem types,
651 *Nature*.
652 Zhao, M., and S. W. Running (2010), Drought-induced reduction in global terrestrial net
653 primary production from 2000 through 2009, *Science*, *329*(5994), 940.
654
655

ıble 1. Description of parameters used in the model and the prior used in inverse modeling. The value is given if parameter ɛdefined to be a constant and is not used in inverse modeling. Parameters that are per microbial biomass based have differe ıors for dormancy and no-dormancy model. Note that the model simulates top 30 cm of soil.

arameter	Description	Prior / value (Dormancy model)	Prior / value (No-Dormancy model)	Notes and citations
	Maintenance respiration weight, $m_R/(\mu_G+m_R)$, where μ_G is specific growth rate (h^{-1})	[0.01, 0.5]	[0.005, 0.05]	[*G Wang et al.*, 2014b]
	Ratio of dormant microbial maintenance rate to m_R	[0.0005, 0.005]	-	[*G Wang et al.*, 2014b]; [*E Blagodatskaya and Y Kuzyakov*, 2013]
$ı_R$	Specific maintenance rate for active biomass (h^{-1})	[0.001,0.08]	[0.0001, 0.008]	[*G Wang et al.*, 2014b]; [*J P Schimel and M N Weintraub*, 2003]; [*E Blagodatskaya and Y Kuzyakov*, 2013]
ɪs	Half-saturation constant for directly accessible substrate (mgC cm^{-2})	[0.01, 10]	Same	Calculated based on approximate range of SolubleC/SOC ratio of 1e-4~1e-3 [*E A Davidson et al.*, 2012] and reported Ks fo substrate breakdown of 72mg kg^{-1} soil [*X Xu et al.*, 2014]
ɪm	Half-saturation constant for enzymatic decay of SOC (mgC cm^{-2})	[200, 1000]*	Same	Assuming SOC is not at saturation for enzymatic decay [*J P Schimel and M N Weintraub*, 2003]
ʳmax	Maximum SOC decay rate	[1e-4, 5e-3]	Same	Calculated based on the magnitude of litter input C
_prod	Enzyme production rate of active microorganism (h^{-1})	[1e-4, 8e-4]	[1e-5, 8e-5]	[*J P Schimel and M N Weintraub*, 2003] assumes 5% of the C uptake by microorganism is allocated to exoenzyme production (d^{-1}). This is equivalent to an

				hourly rate of 2e-3 h^{-1}; the typical hourly uptake rate in our model is ~0.3 per microbial biomass
_loss	Enzyme loss rate (h^{-1})	[0.0005,0.002]	Same	[*S D Allison et al.*, 2010]; [*J P Schimel and M N Weintraub*, 2003]
_death	Potential rate of microbial death (h^{-1})	[2e-4, 2e-3]	[2e-5, 2e-4]	[*S D Allison et al.*, 2010]; [*X Xu et al.*, 2014];
)10_enz	Temperature effects on enzyme activity (rate change per 10°C increase in temperature). Based on 6% rate increase per °C.	1.79	Same	[*D L Purich*, 2009]
)10_mic	Temperature effects on microbial metabolic activity (rate change per 10°C increase in temperature). Based on 0.65eV activation energy for soils.	[1.5, 3.5]	Same	[*G Yvon-Durocher et al.*, 2012]
'g	True growth yield, or carbon use efficiency	[0.3, 0.7]	Same	[*R L Sinsabaugh et al.*, 2013]
'g_slope	Temperature sensitivity of Yg per °C increase	-0.012	Same	[*D P German et al.*, 2012]
ıitial ctive raction $_0$)	Active proportion of microbial biomass	[0.05, 0.3]	-	[*J T Lennon and S E Jones*, 2011]

Upper bound of 2500 is used for US-MOz due to its high SOC content.

ıble 2. Calibration sites that are used in this study, including 3 sites from northeastern China and 3 AmeriFlux sites from th

terminous USA. Soil properties are based on the total element content or measurements in the top 30 cm of soil.

	Mixed deciduous forest (CN-Mixed)	Oak forest (CN-Oak)	Larch plantation (CN-Lar)	Marys River Fir (US-MRf)	Metolius Intermediate Pine (US-Me2)	Missouri Ozark (US-MOz)
;atitude, ɔngitude [1]	45.33-45.42N, 127.50-127.56E	45.33-45.42N, 127.50-127.56E	45.33-45.42N, 127.50-127.56E	44.65N, 123.55W	44.45N, 121.56W	38.74N, 92.20W
;levation nasl)[1]	400	400	400	263	1253	219
MAT, MAP[1]	2.8°C, 700cm	2.8°C, 700cm	2.8°C, 700cm	9.0°C, 1350mm	10°C, 480mm	12.8°C, 940mm
'egetation [GBP)	Mixed forest	Deciduous broadleaf forest	Deciduous needleleaf forest	Evergreen needleleaf forest	Evergreen needleleaf forest	Deciduous broadleaf fores
)ominant pecies in verstory[1]	*Tilia amurensis* Rupr.; *Juglans mandshurica* Maxim.	*Quercus mongolica* Fisch;	*Larix gmelinii* Rupr.	*Pseudotsuga menziesii* (Mirb.) Franco (Douglas fir)	*Pinus ponderosa* (ponderosa pine)	*Quercus alba* L (white oak), *Q. velutina* Lam. (black oak)
oil type[2]	Sandy loam	Sandy loam	Sandy loam	Sandy loam*	Sandy loam	Silt loam
'lay[2]	-	-	-	-	7	-
and[2]	-	-	-	-	67	-
ilt[2]	-	-	-	-	26	-
oil C:N[3]	13.6	20.6	15.8	23.86 *	23.86	16 *
OC :action (%)[4]	9.7	7.6	4.8	1.2 *	1.2	8 *
;ulk density g cm^{-3})[5]	0.63	0.58	1.01	1.15 *	1.15	1.37
Microbial iomass C mg kg^{-1})[6]	1950	1050	900	-	-	-

Microbial biomass N (mg kg^{-1})[6]	210	110	90	-	-	-
Microbial C:N[6]	9.3	9.6	10	-	-	-
MIC/SOC[6]	0.013	0.011	0.009	0.016	0.016	0.99
Citations	1.[*C Wang et al.*, 2006] 2-3.[*M Fu et al.*, 2009] 4-5.[*J Yang and C Wang*, 2005] 6.[*S Liu and C Wang*, 2010]	1.[*C Wang et al.*, 2006] 2-3.[*M Fu et al.*, 2009] 4-5.[*J Yang and C Wang*, 2005] 6.[*S Liu and C Wang*, 2010]	1.[*C Wang et al.*, 2006] 2-3.[*M Fu et al.*, 2009] 4-5.[*J Yang and C Wang*, 2005] 6.[*S Liu and C Wang*, 2010]	1. [*C K Thomas et al.*, 2009] 6.[*X Xu et al.*, 2013]	1. [*J Irvine and B E Law*, 2002] 2-5. DOI: 10.3334/CDIAC /amf.US-Me2.b 6. Xu et al., 2013	1-2. [*L Gu et al.*, 2006] 5. DOI: 10.3334/ CDIAC/amf.US -Moz.b 6. Xu et al., 2013

Values are not reported in literature, average of the same ecosystem type are used for substitution

663 **Table 3.** Model evaluation statistics from ensemble inverse parameter estimation for
664 dormancy and no-dormancy model at the 6 temperate forest sites. NS is the Nash-
665 Sutcliffe model efficiency coefficient. The significance of the difference of metrics
666 between the two models is tested using paired t-test.

Model	RMSE (S.D.) (mg C cm^{-2} h^{-1})	Adjusted-R^2 (S.D.)*	NS coefficient	Seasonal MIC amplitude (mg C cm^{-2})**
Dormancy model:				
CN-Mixed	0.0062	0.55	-0.25	2.8
CN-Oak	0.0021	0.51	-0.02	2.5
CN-Lar	0.0016	0.54	0.53	1.3
US-MRf	0.0011	0.76	0.75	1.7
US-Me2	0.0012	0.63	0.55	3.2
US-MOz	0.0018	0.56	0.43	2.3
No-dormancy model:				
CN-Mixed	0.0065	0.36	-0.29	5.3
CN-Oak	0.0056	0.48	-0.02	5.2
CN-Lar	0 .002	0.52	0.48	4.5
US-MRf	0.0009	0.73	0.71	1.3
US-Me2	0.0015	0.63	0.48	3.9
US-MOz	0.0093	0.32	-0.68	3.5

667 *: Metrics are significantly different between the two models at $p<0.1$

668 **: Metrics are significantly different between the two models at $p<0.05$

biomass (r) and soil heterotrophic respiration (R_H), and soil properties, soil temperature, and soil volumetric moisture content for temperate forest.

Soil physical and environmental factors	Dormancy Model				No-dormancy Model
	r (summer)	r (winter)	r (annual mean)	R_H	R_H
Bulk density (g cm^{-3})	-	-	-	-0.36***	-0.37***
Particle density (g cm^{-3})	-	-	-	-0.48***	-0.49***
Organic C content (mg cm^{-2}) in the top 30 cm	0.04*	0.14***	0.11***	0.89***	0.90***
Soil C:N ratio	0.41***	0.21***	0.34***	0.32***	0.27***
Lillterfall C input (gC m^{-2} yr^{-1})	-	-	-	0.06**	0.02
Annual mean soil temperature at 10cm	0.03	0.17***	0.08***	0.19***	0.16***
Annual mean soil volumetric moisture at 10cm	0.06***	0.04	0.04**	0.14***	0.15***
Seasonal amplitude of soil temperature (summer - winter)	0.10***	0.09***	0.03	-	-
Seasonal amplitude of soil volumetric moisture (summer - winter)	0.19***	0.13***	0.06**	-	-
Soil volumetric moisture in summer	0.05**	0.07**	0.06**	-	
Soil volumetric moisture in winter	0.06	0.06**	0.02	-	-

* Significant at P<0.1; ** significant at P<0.05; ***significant at P<0.001

673 **Figure Captions**

674 **Figure 1.** Modeled SOC decomposition dynamics at an Ameriflux ponederosa pine forest
675 in the United States (US-Me2). Subplot (a) – (d) are outputs from the dormancy model;
676 (e), (g), (h) are outputs from the no-dormancy model. (f) is the measured soil temperature
677 and volumetric moisture content at the site.

678 **Figure 2.** Modeled SOC decomposition dynamics at the larch plantation in northeastern
679 China (CN-Lar). Note that this is a trenched plot. Subplot (a) – (d) are outputs from the
680 dormancy model; (e), (g), (h) are outputs from the no-dormancy model. (f) is the
681 measured soil temperature and volumetric moisture content at the site.

682 **Figure 3.** Parameters that are obtained after inverse modeling for dormancy model at all
683 6 sites. DB indicates deciduous broadleaf forest; EN indicates evergreen needleleaf
684 forest.

685 **Figure 4.** Simulated spatial pattern soil R_H and the MIC/SOC ratio of the two models.

686 **Figure 5.** The spatial pattern of the active proportion of microbial biomass in summer
687 and winter, and the C:N ratio of soil organic matter of the temperate forest latitudinal
688 band (25°N-50°N).

689 **Figure 6.** Temporal correlation (Pearson correlation coefficient) at each grid cell between
690 (a) active proportion of microbial biomass and soil volumetric moisture content, (b)
691 active proportion of microbial biomass and soil temperature, and (c) soil temperature and
692 moisture content.

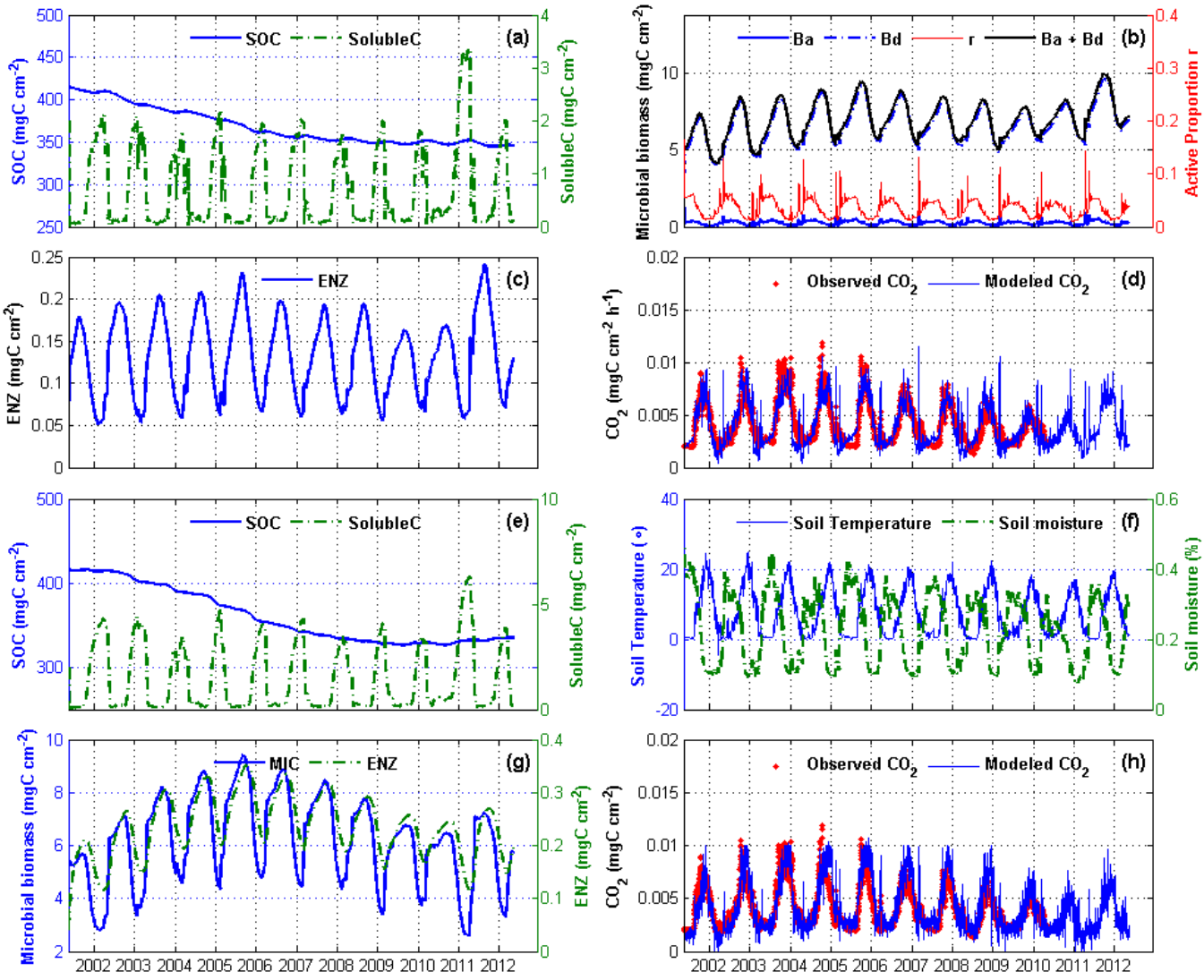

693

694 **Figure 1**

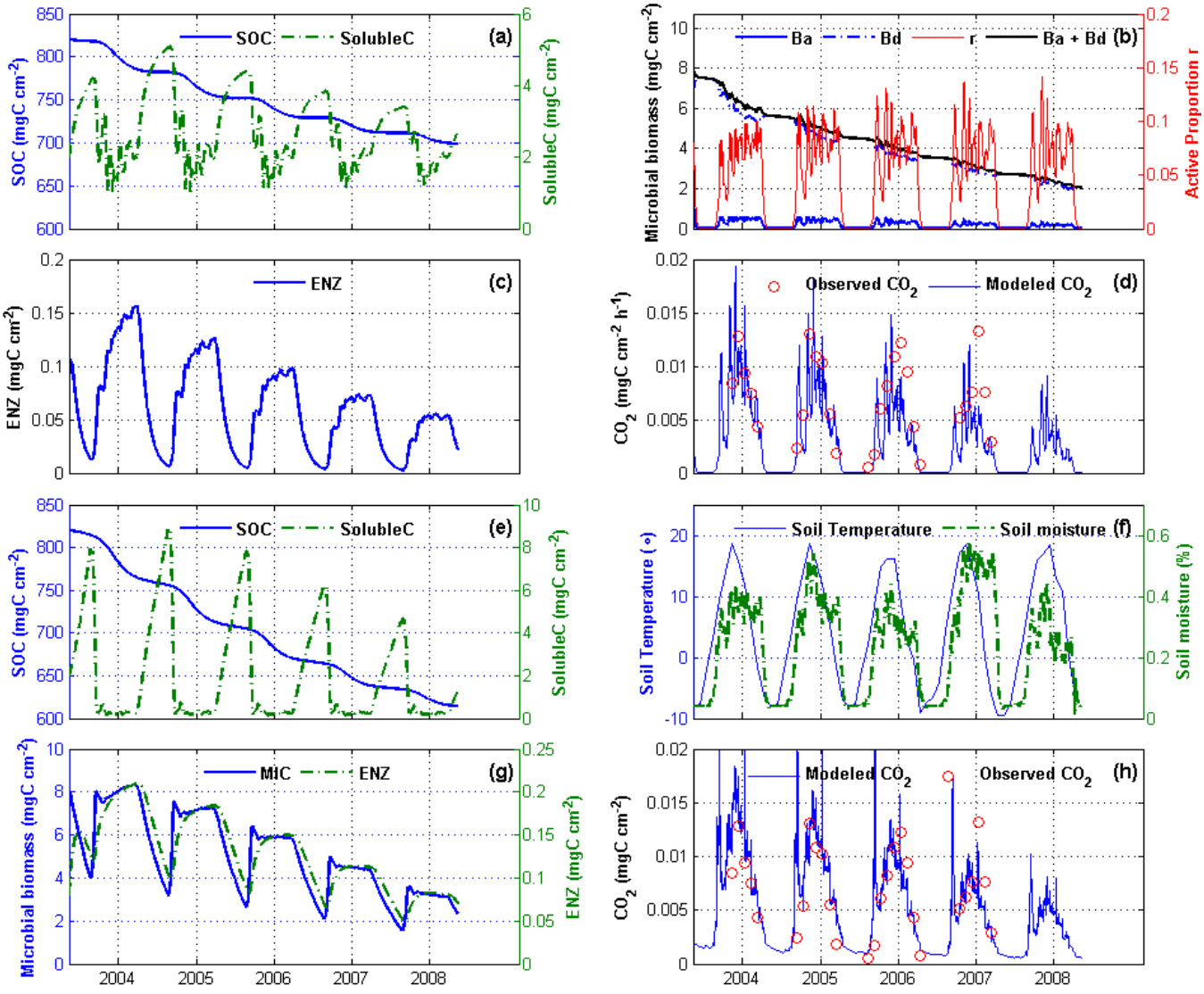

695

696 **Figure 2**

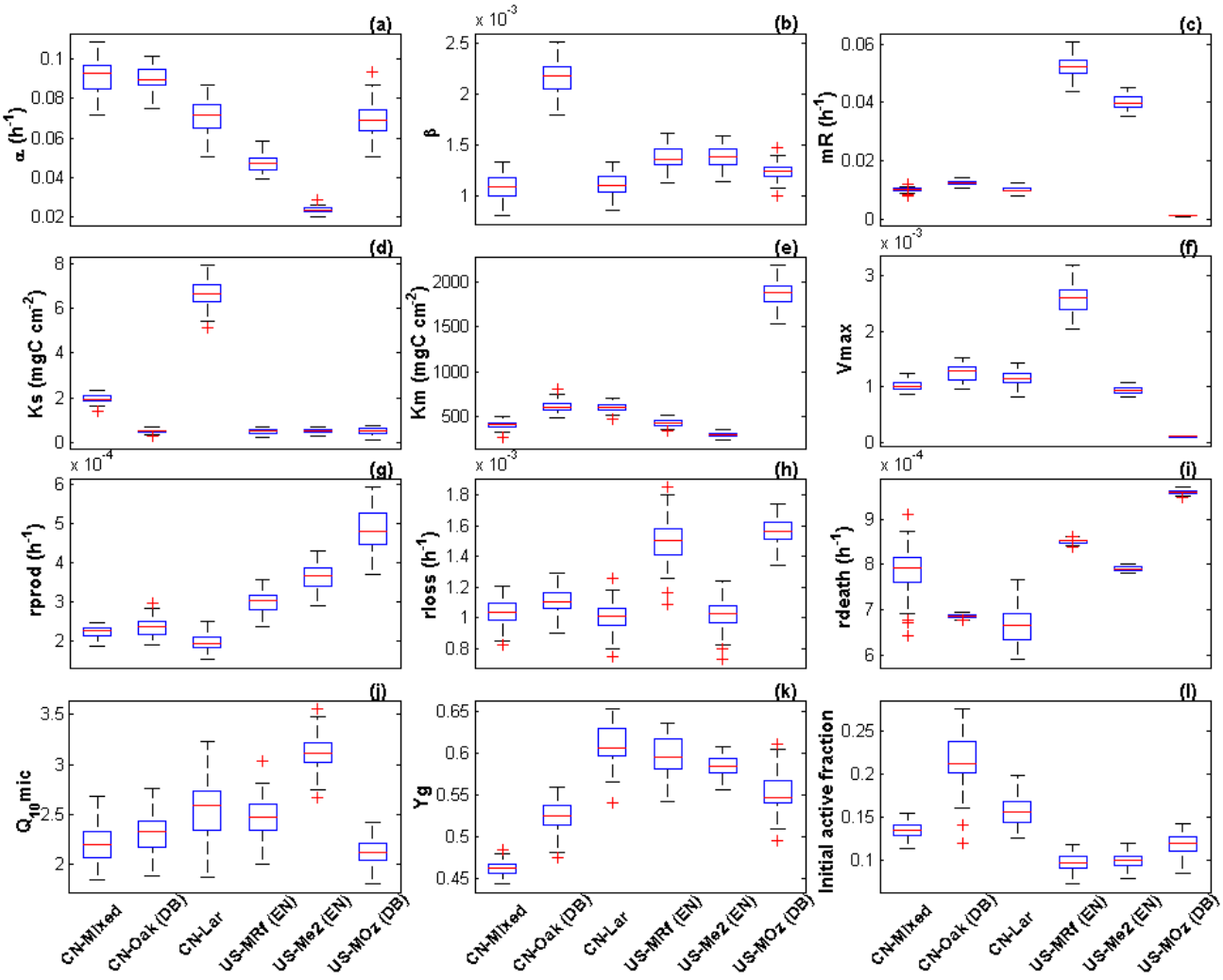
(a)
α (h-1)
(b)
x 10-3
β
(c)
mR (h-1)
(d)
Ks (mgC cm-2)
(e)
Km (mgC cm-2)
(f)
x 10-3
Vmax
(g)
x 10-4
rprod (h-1)
(h)
x 10-3
rloss (h-1)
(i)
x 10-4
rdeath (h-1)
(j)
Q10mic
(k)
Yg
(l)
Initial active fraction
CN-Mixed
CN-Oak (DB)
CN-Lar
US-MRf (EN)
US-Me2 (EN)
US-MOz (DB)

Figure 3

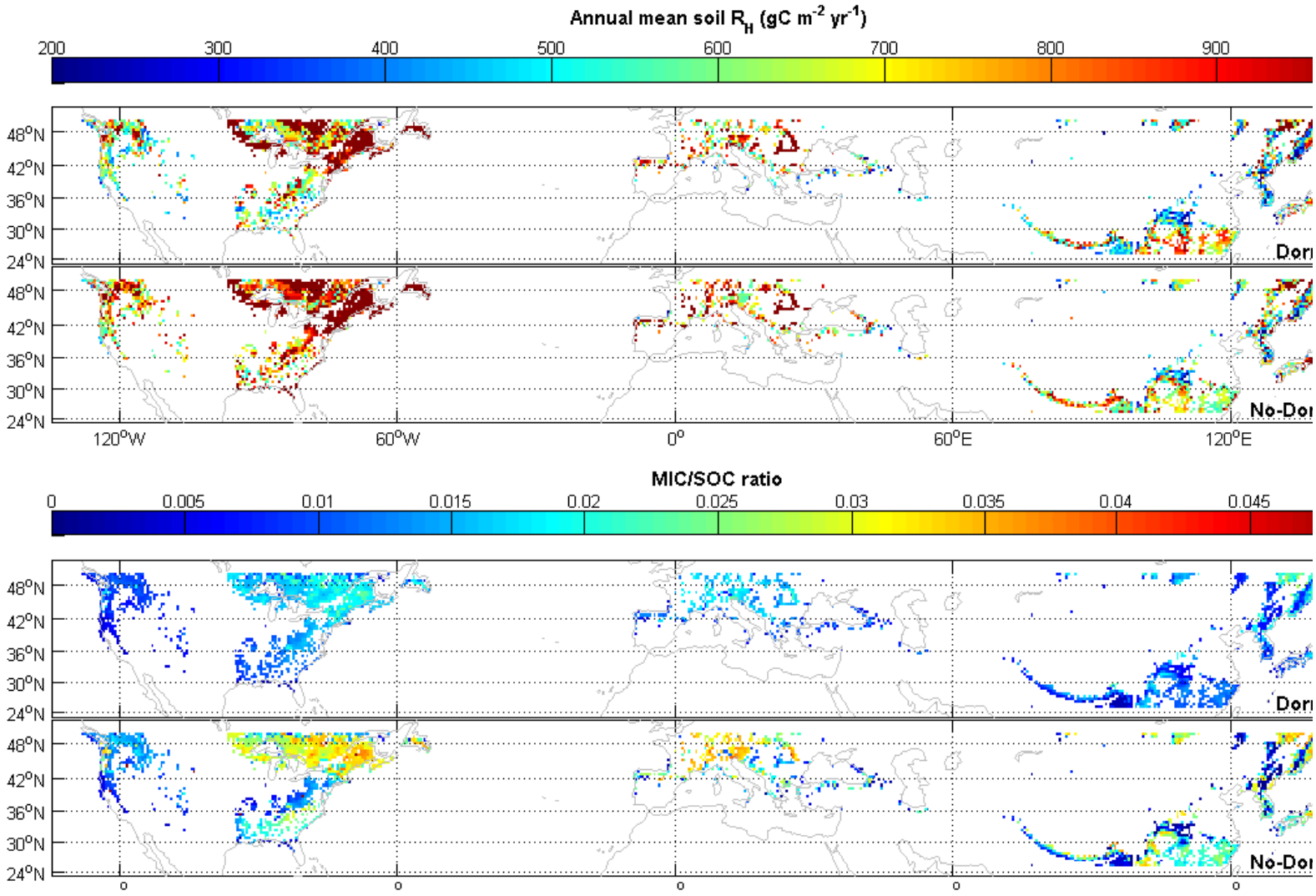
Annual mean soil R_H (gC m^{-2} yr^{-1})
200
300
400
500
600
700
800
900
48°N
42°N
36°N
30°N
24°N
Dor
No-Dor
120°W
60°W
0°
60°E
120°E
MIC/SOC ratio
0
0.005
0.01
0.015
0.02
0.025
0.03
0.035
0.04
0.045

gure 4

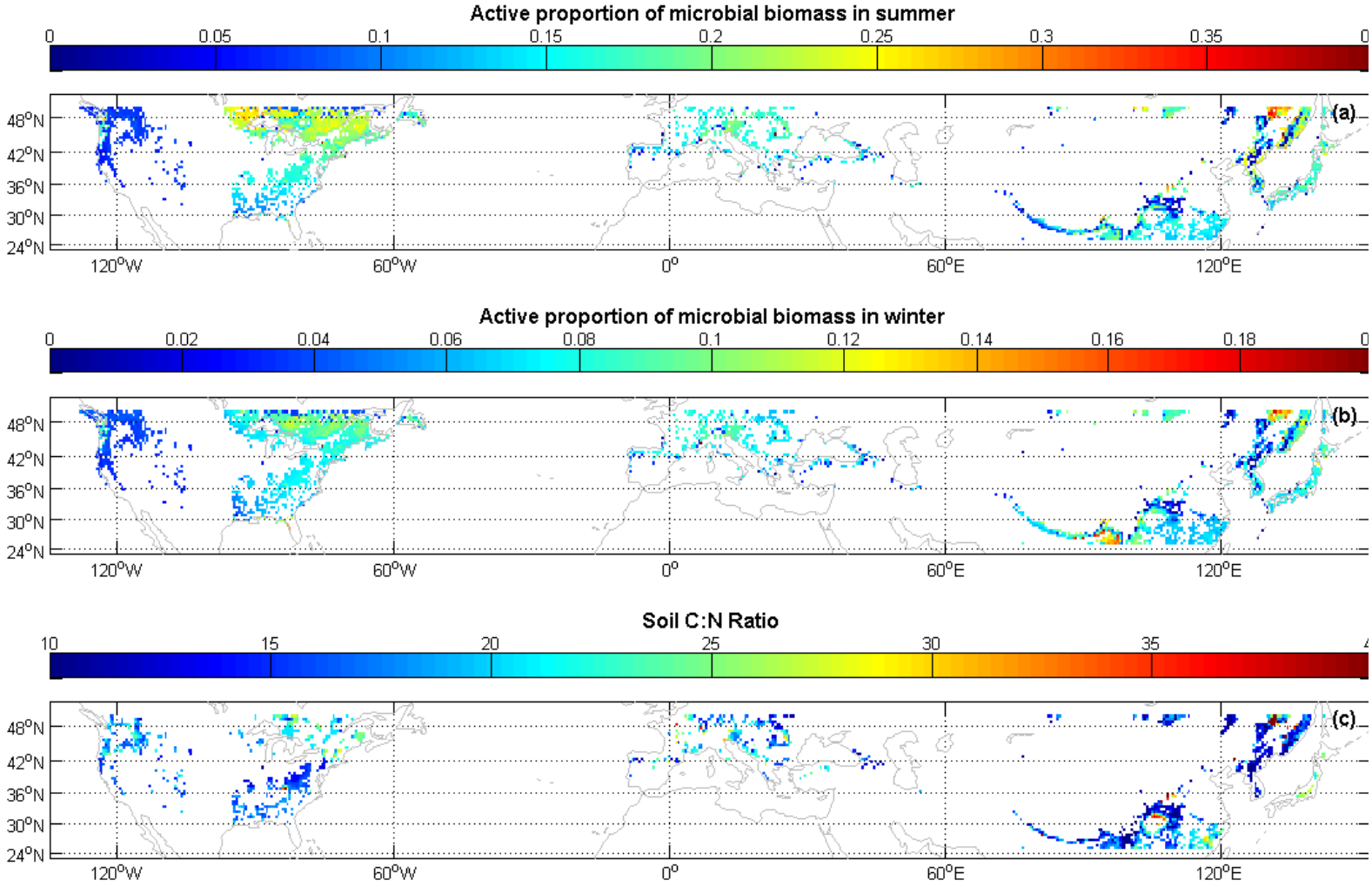
Active proportion of microbial biomass in summer
0
0.05
0.1
0.15
0.2
0.25
0.3
0.35
(a)
48°N
42°N
36°N
30°N
24°N
120°W
60°W
0°
60°E
120°E
Active proportion of microbial biomass in winter
0
0.02
0.04
0.06
0.08
0.1
0.12
0.14
0.16
0.18
(b)
Soil C:N Ratio
10
15
20
25
30
35
(c)

gure 5

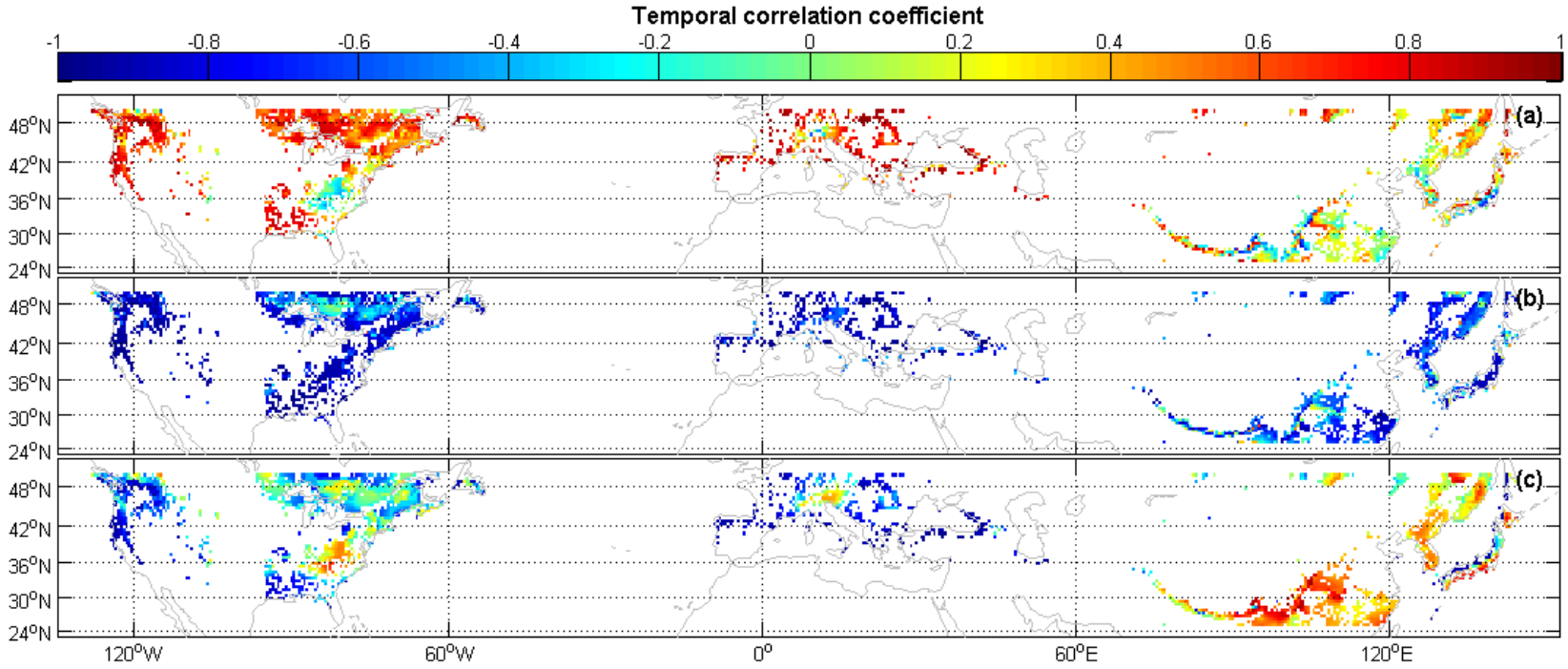

703

704 **Figure 6**